Fluid-Structure Interaction in Microchannel Using Lattice Boltzmann Method and Size-Dependent Beam Element

V. Esfahanian*, E. Dehdashti and A. M. Dehrouyeh-Semnani

School of Mechanical Engineering, University of Tehran, Tehran 14395-515, Iran

Abstract. Fluid-structure interaction (FSI) problems in microchannels play prominent roles in many engineering applications. The present study is an effort towards the simulation of flow in microchannel considering FSI. Top boundary of the microchannel is assumed to be rigid and the bottom boundary, which is modeled as a Bernoulli-Euler beam, is simulated by size-dependent beam elements for finite element method (FEM) based on a modified couple stress theory. The lattice Boltzmann method (LBM) using D2Q13 LB model is coupled to the FEM in order to solve fluid part of FSI problem. In the present study, the governing equations are non-dimensionalized and the set of dimensionless groups is exhibited to show their effects on micro-beam displacement. The numerical results show that the displacements of the micro-beam predicted by the size-dependent beam element are smaller than those by the classical beam element.

AMS subject classifications: 74F10, 74N15, 74A60, 80M10, 76T99

Key words: Fluid-structure interaction, microchannel, lattice Boltzmann method, size-dependent beam element.

1 Introduction

Due to the recent rapid development of micro flow devices applied in micro-total-analysis-systems (*m*-TAS) and micro-electro-mechanical systems (MEMS), modeling and simulation methods for flows in such micro geometries have been of great interest in the society of computational physics [1]. The design of stirrers, extruders and injection systems in process engineering or artical heart valves and blood vessels in medicine require the consideration of the bidirectional interaction between fluid and structure as well.

---

*Corresponding author.
Email: evahid@ut.ac.ir (V. Esfahanian), iman.dehdashti@ut.ac.ir (E. Dehdashti), a.m.dehrouye@ut.ac.ir (A. M. Dehrouyeh-Semnani)

In general, two approaches to solve FSI problems exist: The monolithic approach [2] discretizes the two separate domains with a similar discretization scheme and solves the resulting, coupled system of equations within one solver. The compatibility conditions at the interface are treated inherently within this system of equations. By contrast, the partitioned approach [3] uses separate solvers for the fluid and the structural system. Strong coupling methods [4] as well as loose coupling methods [5] exist. In the partitioned solution, the solvers need to communicate physical properties of their mutual boundary to fulfill the interface conditions. Each domain may utilize any type of discretization considered efficient for its field.

Several numerical techniques have been also developed for FSI problems using the macroscopic continuity and momentum equations for flow field. Some of them used FEM for both fluid and structure analyses [6,7], and some others used coupled FEM and the boundary element method [8,9]. Most of those studies considered potential flow for FSI. Viscous flow considered in blood flow using FEM [10,11].

In microscale applications, microstructure-dependent size effects are often observed [12]. Beam models based on classical elasticity are not capable of describing such size effects due to the lack of a material length scale parameter. This motivated the development of beam models using higher-order (non-local) continuum theories that contain additional material constants. In view of the difficulties in determining microstructure-dependent length scale parameters [13] and the approximate nature of beam theories, non-classical beam models involving only one material length scale parameter are desirable. One such model has recently been developed for the Bernoulli-Euler beam by Park and Gao [14] using a modified couple stress theory proposed by Yang et al. [15], which contains only one material length scale parameter. The modified couple stress theory was employed to develop a size-dependent beam element able to predict the size-dependency observed in microbeams by Kahrobaiyan et al. [16].

The Navier-Stokes (macroscopic momentum) equations are, no longer applicable to micro flows (levels of moderately high Knudsen number) and the flow physics in such flows is described by the Boltzmann equation (BE) of the gas kinetic theory [17]. Moreover, an advantage of the LBM compared to conventional computational fluid dynamics (CFD) solvers is the local availability of the stress tensor. For example, problems such as multiphase flows [18], turbulent flow [19], and thermal flow [20] could be handled effectively using the LBM. The first LB algorithm for an interaction problem between a fluid and rigid obstacles has been developed by Ladd [21,22] for the simulation of particulate suspensions. An application of the LBM to FSI was the case with flow around rigid structures as appeared in articial heart-valve geometries [23]. Moreover, Coupling of LBM to FEM for FSI application was undertaken in the staggered manner for D2Q9 LB model [24]. The D2Q9 LB model can only capture the basic feature at sufficiently small Knudsen numbers. Higher-order LB method improves the accuracy in micro flows (finite Knudsen number), as had been compared with the standard LB method. Transient bidirectional FSI problem was investigated with geometrically non-linear structural deflections [25]. However, to the best knowledge of the authors, there were few efforts to
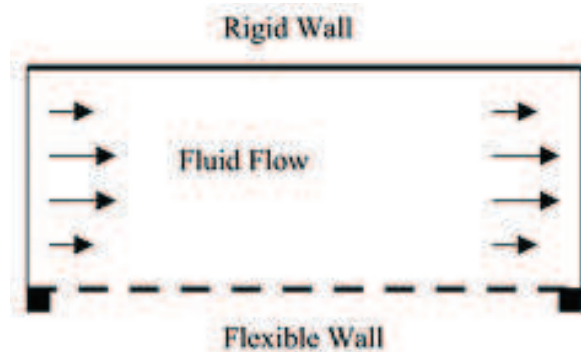
Figure 1: Flow between rigid and flexible walls in microchannel.

couple the LBM to the FEM to solve the fluid and flexible structure interaction problems in microscale considering microstructure-dependent size effects in micro-beam.

In the present study, two-dimensional flow is solved in microchannel as shown in Fig. 1. To simulate microchannel, D2Q13 LB model is applied using the staggered manner to couple the LBM and the FEM to solve FSI problem. Top boundary is assumed to be rigid while the bottom boundary is considered to be flexible. The flexible boundary is modeled as a Bernoulli-Euler beam with clamped at both end points. The modified couple stress theory is used to solve the dynamic problem of Bernoulli-Euler beam. In the present study, the governing equations are non-dimensionalized and the set of dimensionless groups is presented to show their effects on micro-beam displacement. The numerical results show that the displacements of the micro-beam predicted by the size-dependent beam element are smaller than those by the classical beam element.

2 Lattice Boltzmann method

The LBM was originated from lattice gas (LG) automata [26], which are discrete particle kinetics based on discrete time and lattice spaces. The LB equation is expressed as:

$$f_i(\mathbf{x}+\mathbf{e}_i\Delta t, t+\Delta t) - f_i(\mathbf{x}, t) = \Omega_i(f(\mathbf{x}, t)), \tag{2.1}$$

where $f_i(\mathbf{x}, t)$ denotes the probability of finding a particle at lattice site $\mathbf{x}$ and time t, which moves with the local particle velocity $\mathbf{e}_i$. Furthermore, Δt is the time increments, and Ω_i is the collision operator for the rate of change of f_i resulting from collision, and it depends only on the local value of $f_i(\mathbf{x}, t)$.

In Eq. (2.1), the local particle velocity $\mathbf{e}_i$ is discrete in the given lattice. For a D2Q13 lattice model as shown in Fig. 2, the discrete velocities for the thirteen possible directions
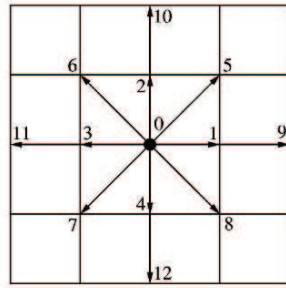
Figure 2: LB model with 13 discrete velocity vectors.

are:

$$e_0 = 0,$$

$$e_i = \left[\cos\left(\frac{((i-1)\pi)}{2}\right),\sin\left(\frac{((i-1)\pi)}{2}\right)\right]c, \qquad\qquad i=1-4,$$

$$e_i = \left[\cos\left(\frac{((i-5)\pi)}{2}+\frac{\pi}{4}\right),\sin\left(\frac{((i-5)\pi)}{2}+\frac{\pi}{4}\right)\right]\sqrt{2}c, \qquad i=5-8,$$

$$e_i = \left[\cos\left(\frac{((i-1)\pi)}{2}+\frac{\pi}{4}\right),\sin\left(\frac{((i-1)\pi)}{2}+\frac{\pi}{4}\right)\right]2c, \qquad i=9-12,$$

where $c = \Delta x / \Delta t$ and Δx is the lattice spacing step. For the BGK model [27], the collision operator is expressed as:

$$\Omega_i = -\frac{f_i(\mathbf{x},t) - f_i^{(eq)}(\mathbf{x},t)}{\tau},$$

where τ is the relaxation time and $f_i^{(eq)}$ denotes the local equilibrium distribution. This local equilibrium is derived from the Maxwell-Boltzmann equilibrium distribution. The equilibrium distribution defined as:

$$f_i^{(eq)} = \rho w_i \left(1 + \frac{e_{ik}u_k}{c_s^2} + \frac{(e_{ik}u_k)^2}{2c_s^2} - \frac{u_k u_k}{2c_s^2} + \frac{(e_{ik}u_k)^3}{2c_s^6} - \frac{3(e_{ik}u_k)(u_k u_k)}{2c_s^4}\right), \qquad (2.2)$$

in which ρ is the fluid density, u is the fluid velocity, $c_s = c/\sqrt{2}$ is the lattice speed of sound. Where weight coefficients in Eq. (2.2) are as:

$$w_0 = \frac{3}{8};$$

$$w_i = \frac{1}{12}, \qquad i=1-4;$$

$$w_i = \frac{1}{16}, \qquad i=5-8;$$

$$w_i = \frac{1}{96}, \qquad i=9-12.$$

The fluid density ρ and momentum density $\rho\mathbf{u}$ are expressed as:

$$\rho = \sum_{i=0}^{12} f_i, \qquad \rho\mathbf{u} = \sum_{i=0}^{12} \mathbf{e}_i f_i.$$

Furthermore, it can be shown that the pressure fluid p and the kinematic viscosity ν derived from the Boltzmann BGK equation through the Chapman-Enskog expansion is:

$$p = c_s^2 \rho, \qquad \nu = \Delta t c_s^2 (\tau - 0.5).$$

In equilibrium, the conservation of mass and momentum is satisfied at each lattice:

$$\sum_{i=0}^{12} \Omega_i = 0, \qquad \sum_{i=0}^{12} \Omega_i \mathbf{e}_i = 0.$$

3 Finite element method

The flexible boundary is modeled as a micro-beam with clamped at both end points. The cross-section of the micro-beam is rectangular. The total length of the microscale beam is L_x, cross-section height and width of that is h, l_y, respectively. The Cartesian axes for beam analysis are established, as shown in Fig. 3. The dynamic governing equation of the beam in terms of $w(\mathbf{x},t)$ is given by

$$(EI + GAl^2)\frac{\partial^4 w}{\partial x^4} + \rho A \frac{\partial^2 w}{\partial t^2} = q(\mathbf{x},t), \tag{3.1}$$

where $w(\mathbf{x},t)$ is z-component of the displacement vector, I is the usual second moment of cross-sectional area and A is the cross-sectional area of the beam, E, G are the Young's modulus and the shear modulus, respectively. q is transverse loading and ρ is the density of the beam material. l is a material length scale parameter.
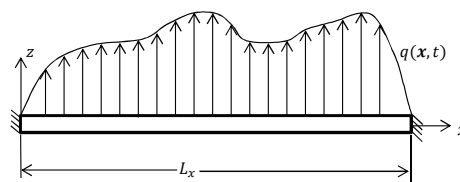

Figure 3: Schematic diagram of Cartesian coordinate system for Bernoulli-Euler beam.

The boundary conditions for solving Eq. (3.1) is considered as:

$$\begin{cases} \dfrac{\partial w(\mathbf{x},t)}{\partial x} = 0 & \text{at } x = 0, L_x, \\ w(\mathbf{x},t) = 0 & \text{at } x = 0, L_x. \end{cases}$$

It can be seen from Eq. (3.1) that the equilibrium relations of the beams are related to two parts: one associated with ρA and EI as in classical beam model and the other associated with GAl^2. Also, it should be emphasized that the current beam model based on the modified couple stress theory contains only one additional material constant besides two classical material parameters. Nevertheless, the presence of l enables the incorporation of the material size features in the new model and renders it possible to explain the size effect [28]. Furthermore, when the size effect is suppressed by letting $l=0$, the new model will reduce to the classical beam model.

When the microstructural effect is considered, substituting $(EI)^\star$ instead of $EI+GAl^2$, Eq. (3.1) can be written as:

$$(EI)^\star \frac{\partial^4 w}{\partial x^4} + \rho A \frac{\partial^2 w}{\partial t^2} = q(\mathbf{x},t),$$ (3.2)

which is identical to the governing equation derived in macrosclae beam with equivalent flexural rigidity $(EI)^\star$.

4   Coupling of LBM and FEM

of the boundary conditions at the fluid-structure interface is given as:

$$v = \frac{\partial w}{\partial t},$$

where w is z-component of the structural displacement vector at the fluid-structure boundary and this equation states the continuity of velocity at the boundary. Furthermore, the continuity of traction at the fluid-structure boundary is expressed as:

$$\sigma_{kl}^f n_l = \sigma_{kl}^s n_l.$$

An advantage of the LBM compared to conventional CFD solvers is the local availability of the stress tensor [24]. The stress tensor σ_{kl}^f with scalar pressure is:

$$\sigma_{kl}^f = -p\delta_{kl} + S_{kl},$$ (4.1)

S_{kl} is computed from the non-equilibrium part of the distributions and δ is the Kronecker-delta [29].

$$S_{kl} = \left(1 - \frac{1}{2\tau}\right) \sum_{i=0}^{12} f_i^{(neq)} \left(e_{ik} e_{il} - \frac{1}{2}\mathbf{e}_i \mathbf{e}_i \delta_{kl}\right).$$

Coupling of LBM to FEM for FSI application is undertaken in the staggered manner. In other words, the LBM is applied to the fluid domain using the velocity boundary conditions obtained from the FEM at the fluid-structure interface. Then, the fluid traction

is computed from the LBM at the fluid-structure boundary. The traction is applied to the structural finite element analysis. This solution cycle is continued until the solutions for the fluid and structure became compatible at the interface boundaries.

A procedure to apply the fluid-structure interface velocity boundary condition to the LBM is described below. First of all, boundary condition scheme is applied to the fluid-structure boundary lattice points of the LBM. Then, the local particle distribution f_i is further modified as follows to maintain the velocity continuity at the fluid-structure boundary. Let $\dot{w}_x$ and $\dot{w}_y$ be the structural velocity components along the x- and y-axis at the fluid-structure interface. The particle distribution is revised as follows:

$$f_1 = f_1 + \frac{\dot{w}_x}{2}, \qquad f_2 = f_2 + \frac{\dot{w}_y}{2}, \qquad f_3 = f_3 - \frac{\dot{w}_x}{2},$$

$$f_4 = f_4 - \frac{\dot{w}_y}{2}, \qquad f_5 = f_5 + \frac{2\dot{w}_x}{3} + \frac{2\dot{w}_y}{3}, \qquad f_6 = f_6 - \frac{2\dot{w}_x}{3} + \frac{2\dot{w}_y}{3},$$

$$f_7 = f_7 - \frac{2\dot{w}_x}{3} - \frac{2\dot{w}_y}{3}, \qquad f_8 = f_8 + \frac{2\dot{w}_x}{3} - \frac{2\dot{w}_y}{3}, \qquad f_9 = f_9 + 4\dot{w}_x,$$

$$f_{10} = f_{10} + 4\dot{w}_y, \qquad f_{11} = f_{11} - 4\dot{w}_x, \qquad f_{12} = f_{12} - 4\dot{w}_y.$$

When the traction was computed from the LBM using Eq. (4.1), then the finite element analysis by using Eq. (3.2) is conducted using the following equation:

$$[M]\{\ddot{w}\} + [K]\{w\} = \{F\} + \{P\},$$

where $[M]$ and $[K]$ which is obtained for micro-finite-element model by Kahrobaiyan et al. [16], are the finite element mass and stiffness matrices, respectively. Furthermore, $\{F\}$ is the external force vector and $\{P\}$ is the force vector resulting from the FSI as expressed below:

$$\{P\} = \sum \int_{\Gamma_{int}} [N]^T \{r\} d\Gamma.$$

Here, $[N]$ is the matrix composed of finite element shape functions over the interface element boundary Γ_{int}, and $\{r\}$ is the traction vector. The summation is over the total number of finite element boundaries at the fluid-structure interface.

5 Numerical results

The departures from the local equilibrium are measured by the Knudsen number, namely the ratio of molecular mean free path, l_m, to the shortest hydrodynamic scale, l_h:

$$Kn = \frac{l_m}{l_h}.$$

Table 1: Definition of dimensionless groups.

Dimensionless group	Formula	Name
Π_1	$\dfrac{L_x}{h}$	Length-to-height ratio of the beam
Π_2	$\dfrac{h}{l}$	Material length-to-height ratio of the beam
Π_3	$\dfrac{p}{E}$	Pressure-to-Young's modulus ratio
Π_4	$\dfrac{u_0 l_z}{\nu}$	Reynolds number (Re)
Π_5	$\sqrt{\dfrac{\rho_s}{E}}\, u_0$	Elastic number
Π_6	$\dfrac{\rho_f}{\rho_s}$	Density ratio

The Knudsen number is tuned by changing the value of the viscosity, according to the expression [30]:

$$Kn = \frac{\nu}{c_s l_z}.$$

The *Kn* number in the present work is considered very small so that the fluid field can be solved with the no-slip boundary conditions [31]. But the effect of micro-beam is considered in structural simulation by using size-dependent beam element.

In the present study, Two-dimensional flow in microchannel is solved. D2Q13 LB model using a technique to couple the LBM and the FEM is applied to solve FSI problems. Top boundary is assumed to be rigid while the bottom boundary is considered being flexible. The flexible boundary is modeled as a Bernoulli-Euler beam with clamped at both end points. The non-equilibrium extrapolation boundary condition is used for the flow field [32].

Writing non-dimensional forms of the governing equations, can yield insight into the underlying physical phenomena, and indicate which forces are dominant. If is exist two dynamically similar but different property flows, the equations would only yield the same mathematical results if the two flows had the same values for the dimensionless groups. In the present study, the governing equations are non-dimensionalized and the set of dimensionless groups as shown in Table 1, is exhibited to show their effects on micro-beam displacement. Where p, u_0 and ν are flow pressure, inlet flow velocity and viscosity of fluid, respectively. ρ_f, ρ_s are the fluid and solid density, respectively and l_z is the height of microchannel.

Effects of Π_2 to Π_6 is studied on displacement of micro-beam as follows. As fluid flows, the flexible beam vibrates up and down. Time history of the vibrational motion of the flexible beam at center is shown in follow figures. In all plots, displacements are non-dimensionalized with respect to the lattice grid size while time is normalized in terms of the time increment. Fig. 4 indicates the displacement is increased, by increasing Π_2 and
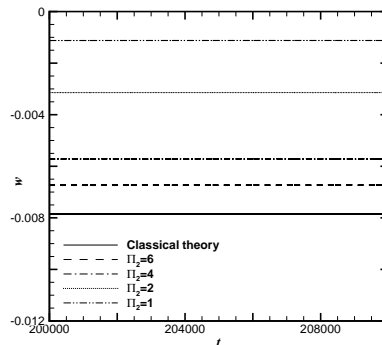
Figure 4: Time history plot of the displacement at the center of the micro-beam with $Re = 50$, $\Pi_3 = 5 \times 10^{-7}$, $\Pi_5 = 0.04$, $\Pi_6 = 0.1$ and different Π_2.

that converges to result for classical model by more increasing Π_2. The vibrations are invisible in Fig. 4, magnifying that the vibrations are plotted in Fig. 5.

When Π_3 is increased means the flow pressure which forcing to the boundary is increased or the micro-beam has less Young's modulus, that both of them make more displacement that can be seen in Fig. 6. As shown in Fig. 7, when the Π_5 is increased amplitude of vibrations is increased that means for micro-beam with known properties, when the flow velocity is increased, amplitude of vibrations is increased. The displacement for different Π_6 is shown in Fig. 8, which indicates amplitude of vibrations is decreased, when the Π_6 is increased. The Reynolds number which is a important property of flow that determine whether flow is formed in a laminar or turbulent way is now considered. Fig. 9 shows the displacement in different Reynolds numbers.

At low Reynolds number laminar flow is steady, but if the Reynolds number be more increased interaction between flow and structure can cause unsteady laminar flow as shown in Fig. 10, for Reynolds number equal to 150 using classical theory. The displacement along the Bernoulli-Euler beam at different time steps is also shown in Fig. 11. Moreover, when Π_2 is increased, bending stiffness of micro-beam is decreased. Therefore, using lesser Π_2, fluid flow which was unsteady (see Fig. 10) can be steady as shown in Fig. 12, using Π_2 equal to 1.

6 Conclusions

A coupling is used for FSI application using LBM for the fluid domain and FEM for the structural domain. Higher-order LB method improves the accuracy in micro flows (finite Knudsen number), as had been compared with the standard LB method. D2Q13 LB model is applied using the staggered manner to couple the LBM and the FEM to solve microscale FSI problem. A size-dependent beam element for the Bernoulli-Euler beam is considered which employ a modified couple stress theory [16]. In modified couple stress theory, one material length scale parameter is included to capture the size effect, unlike
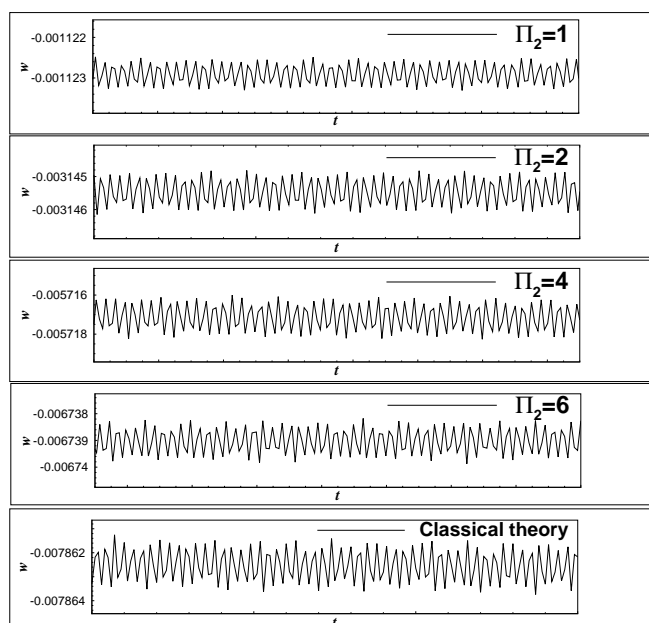
Figure 5: Magnified displacement at the center of the micro-beam with $Re = 50$, $\Pi_3 = 5 \times 10^{-7}$, $\Pi_5 = 0.04$, $\Pi_6 = 0.1$ and different Π_2.
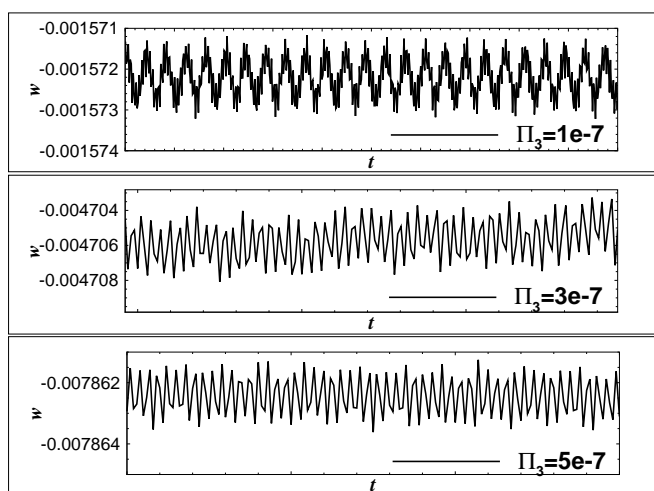

Figure 6: The displacement at the center of the micro-beam with $Re = 50$, $\Pi_2 = 0$, $\Pi_5 = 0.04$, $\Pi_6 = 0.1$ and different Π_3.

the classical Bernoulli-Euler beam theory.

    The numerical results show that the displacements of the micro-beam predicted by the size-dependent beam element are smaller than those by the classical beam element. Moreover, it is found that when Reynolds number is increased considering the classical
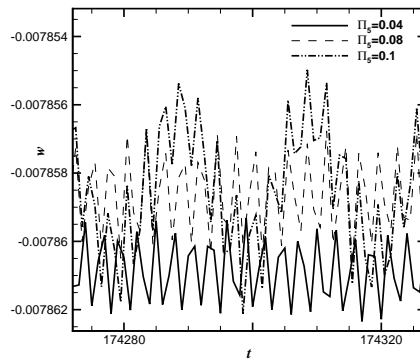
Figure 7: The displacement at the center of the micro-beam with $Re=50$, $\Pi_2=0$, $\Pi_3=5\times10^{-7}$, $\Pi_6=0.1$ and different Π_5.
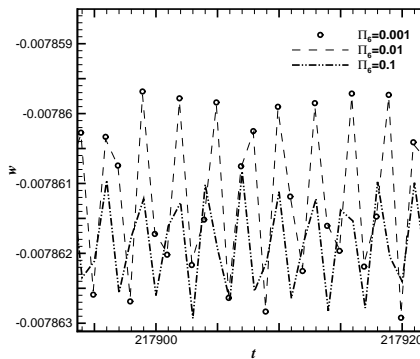

Figure 8: The displacement at the center of the micro-beam with $Re=50$, $\Pi_2=0$, $\Pi_3=5\times10^{-7}$, $\Pi_5=0.04$ and different Π_6.

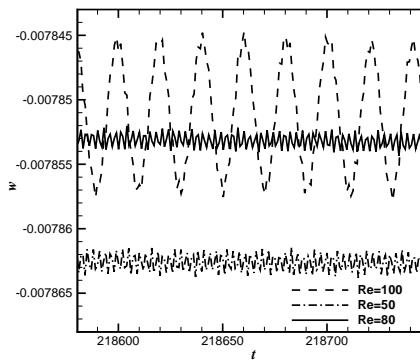

Figure 9: The displacement at the center of the micro-beam with $\Pi_2=0$, $\Pi_3=5\times10^{-7}$, $\Pi_5=0.04$, $\Pi_6=0.1$ and different Re.

element, flow will be unsteady, but considering the non-classical element with enough small Π_2, the flow could be steady. In the other words, the micro-beam will be more stiffness considering a size-dependent beam element based on the modified couple stress
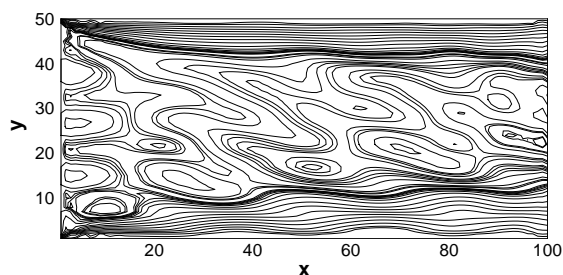
Figure 10: The horizontal velocity contours of the unsteady laminar flow with classical theory and $Re = 150$, $\Pi_3 = 5 \times 10^{-7}$, $\Pi_5 = 0.04$ and $\Pi_6 = 0.1$.
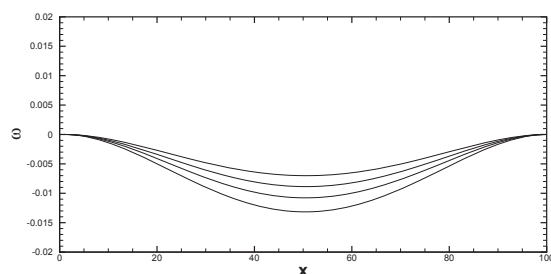

Figure 11: The displacement along the Bernoulli-Euler beam at different time steps with classical theory and $Re = 150$, $\Pi_3 = 5 \times 10^{-7}$, $\Pi_5 = 0.04$ and $\Pi_6 = 0.1$.
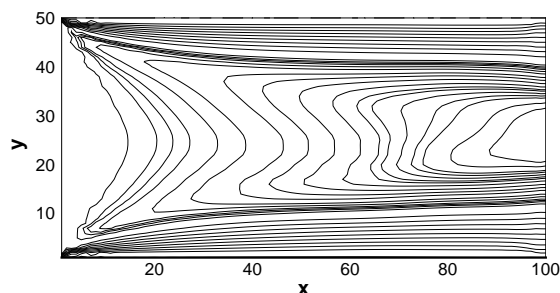

Figure 12: The horizontal velocity contours of the steady laminar flow with $Re = 150$, $\Pi_2 = 1$, $\Pi_3 = 5 \times 10^{-7}$, $\Pi_5 = 0.04$ and $\Pi_6 = 0.1$.

theory. Moreover, the modified distribution functions are obtained using the D2Q13 lattice model. In the future works, the appropriate boundary conditions can be coupled with the present equations to solve the problem with high Kn number, considering the effect of micro in both of fluid and structure simultaneously. The microchannel can be simulated in three-dimensional by applying three dimensional LB model for fluid domain and plate element for the bottom boundary. Moreover, the LBM is useful to solve multiphase problems, hence the present study can be extended to simulate multiphase flows inside or outside flexible structures.

Acknowledgments

References

[1] G. KARNIADAKIS, A. BESKOK AND N. R. ALURU, Microflows and Nanoflows: Fundamentals and Simulation, Springer, 2005.

[2] E. WALHORN, A. KÖLKE, B. HÜBNER AND D. DINKLER, *Fluidstructure coupling within a monolithic model involving free surface flows*, Comput. Struct., 83 (2005), pp. 2100–2111.

[3] P. LETALLEC AND J. MOURO, *Fluid structure interaction with large structural displacements*, Comput. Method. Appl. Mech. Eng., 190 (2001), pp. 3039–3067.

[4] U. KÜTTLER AND W. WALL, *Vector extrapolation for strong coupling fluid-structure interaction solvers*, J. Appl. Mech., 2 (2009), 76.

[5] R. LÖHNER, J. R. CEBRAL, F. F. CAMELLI, J. D. BAUM, E. L. MESTREAU AND O. A. SOTO, *Adaptive embedded/immersed unstructured grid techniques*, Arch. Comput. Method. Eng., 14 (2007), pp. 27–31.

[6] K. J. BATHE, C. NITIKIPAIBOON AND X. WANG, *A mixed displacement-based finite element formulation for acoustice fluid-structure interaction*, Comput. Struct., 56 (1995), pp. 225–237.

[7] Y. W. KWON AND P. M. MCDERMOTT, *Effects of void growth and nucleation on plastic deformation of plates subjected to fluid-structure interaction*, ASME J. Pres. Ves. Technol., 123 (2001), pp. 480–485.

[8] G. C. EVERSTINE AND F. M. HENDERSON, *Coupled finite element/boundary element approach for fluid-structure interaction*, J. Acoust. Soc. Am., 87 (1990), pp. 1938–1947.

[9] J. A. GIORDANO AND G. H. KOOPMANN, *State space boundary element-finite element coupling for fluid-structure interaction analysis*, J. Acoust. Soc. Am., 98 (1995), pp. 363–372.

[10] G. DUBINI, R. PIETRABISSA AND F. M. MONTEVECCHI, *Fluid-structure interaction problems in bio-fluid mechanics: a numerical study of the motion of an isolated particle freely suspended in channel flow*, Med. Eng. Phys., 17 (1995), pp. 609–617.

[11] K. TIENFUAN, L. L. LEE AND L. C. WELLFORD, *Transient fluid-structure interaction in a control valve*, J. Fluids Eng., Trans. ASME, 119 (1997), pp. 354–359.

[12] A. W. MCFARLAND AND J. S. COLTON, *Role of material microstructure in plate stiffness with relevance to microcantilever sensors*, J. Micromech. Microeng., 15 (2005), pp. 1060–1067.

[13] R. MARANGANTI AND P. SHARMA, *A novel atomistic approach to determine strain-gradient elasticity constants: tabulation and comparison for various metals, semiconductors, silica, polymers and the (ir) relevance for nanotechnologies*, J. Mech. Phys. Solids, 55 (2007), pp. 1823–1852.

[14] S. K. PARK AND X. L. GAO, *Bernoulli-Euler beam model based on a modified couple stress theory*, J. Micromech. Microeng, 16 (2006), pp. 2355–2359.

[15] F. YANG, A. C. M. CHONG, D. C. C. LAM AND P. TONG, *Couple stress based strain gradient theory for elasticity*, Int. J. Solids Struct., 39 (2002), pp. 2731–2743.

[16] M. H. KAHROBAIYAN, M. KHAJEHPOUR AND M. T. AHMADIAN, *A size-dependent beam element based on the modified couple stress theory*, ASME Conf. P., 8 (2011), pp. 591–597.

[17] K. SUGA, S. TAKENAKA, T. ITO AND M. KANEDA, *Lattice Boltzmann flow simulation in a combined nanochannel*, Adv. Appl. Math. Mech., 2 (2010), pp. 609–625.

[18] M. R. SWIFT, E. ORLANDINI, W. R. OSBORN AND J. M. YEOMANS, *Lattice Boltzmann simulations of liquid-gas and the binary uid systems*, Phys. Rev. E, 54 (1996), pp. 5041–5052.

[19] M. SOE, G. VAHALA, P. PAVLO, L. VAHALA AND H. CHEN, *Thermal lattice Boltzmann simulations of variable Prandtl number turbulent ows*, Phys. Rev. E , 57 (1998), pp. 4227–4237.

[20] Y. PENG, C. SHU AND Y. T. CHEW, *Simplied thermal lattice Boltzmann model for incompressible thermal ows*, Phys. Rev. E, 68 (2003), 026701.

[21] A. LADD, *Numerical simulations of partiuclate suspensions via a discretized Boltzmann equation: part 1: theoretical foundations*, J. Fluid Mech., 271 (1994), 285.

[22] A. LADD, *Numerical simulations of partiuclate suspensions via a discretized Boltzmann equation. Part 2: numerical results*, J. Fluid Mech., 271 (1994), 311.

[23] M. KRAFCZYK, J. TOLKE, E. RANK AND M. SCHULZ, *Two-dimensional simulation of fluid-structure interaction using lattice-Boltzmann methods*, Comput. Struct., 79 (2001), pp. 2031–2037.

[24] Y. W. KWON, *Development of coupling technique for LBM and FEM for FSI application*, Eng. Comput., 23 (2006), pp. 860–875.

[25] S. KOLLMANNSBERGER, S. GELLER, A. DüSTER, J. TöLKE, C. SORGER, M. KRAFCZYK AND E. RANK, *Fixed-grid uid-structure interaction in two dimensions based on a partitioned Lattice Boltzmann and p-FEM approach*, Int. J. Numer. Meth. Eng., 79 (2009), pp. 817–845.

[26] U. FRISCH, B. HASSLACHER AND Y. POMEAU, *Lattice-gas automata for the Navier-Stokes equations*, Phys. Rev. Lett., 56 (1986), pp. 1505–1508.

[27] P. L. BHATNAGAR, E. P. GROSS, AND M. K. KROOK, *A model for collision process in gases: I: small amplitude processes in charged and neutral one-component system*, Phys. Rev., 94 (1954), pp. 511–525.

[28] S. KONG, S. ZHOU, Z. NIE AND K. WANG, *The size-dependent natural frequency of Bernoulli-Euler micro-beams*, Int J. Eng. Sc., 46 (2008), pp. 427–437.

[29] H-J BUNGARTZ, M. MEHL AND M. SCHäFER, Fluid Structure Interaction II: Modelling, Simulation, Optimization, Springer-Verlag Berlin Heidelberg, 2010, pp. 285–299.

[30] F. TOSCHI AND S. SUCCI, *Lattice Boltzmann method at finite-Knudsen numbers*, Europhys. Lett., 69 (2005), 549.

[31] N. T. NGUYEN, AND S. T. WERELEY, Fundamentals and Applications of Microfluidics, Artech House, Boston, MA, Chapter 2.

[32] Z. L. GUO, C. G. ZHENG AND B. C. SHI, *Non-equilibrium extrapolation method for velocity and pressure boundary conditions in the lattice Boltzmann method*, Chin. Phys. Soc., 11 (2002), 366.